5

SUPPLEMENTARY INFORMATION

10 **Nonstoichiometry, Amorphicity and Microstructural Evolution During Phase Transformations of Photocatalytic Titania Powders**

Suo Hon Lim, Clemens Ritter, Yang Ping, Martin Schreyer and Timothy J. White

TABLE S1: Linear absorption co-efficients for anatase (an), rutile (ru) and amorphous (am) titania as a function of X-ray energy. Following Brindley *(30)* it is expected that polycrystalline diffracting particles experience excessive microabsorption that will invalidate quantitative phase 5analysis when $\mu D > 0.01$. The combination of X-ray energy and particle diameter where reliable Rietveld scale factors can be extracted, provided the phases are distributed homogeneously, is shaded.

E (keV)	mass absorption co-efficient ($cm^2.g^{-1}$)*		linear absorption co-efficient (cm^2)**			D (nm)			
	Ti	O	μ_{an}	μ_{ru}	μ_{am}	400	200	100	50
						$\mu_{an}D$ (for anatase)			
5	683.8	47.9	1707.9	1823.77	1587.75	0.068	0.034	0.017	0.009
6	432.3	27.7	1076.43	1149.46	1000.7	0.043	0.022	0.011	0.005
7	317.3	19.67	789.02	842.55	733.51	0.032	0.016	0.008	0.004
8	202.3	11.63	501.23	535.23	465.97	0.020	0.010	0.005	0.003
9	156.5	8.79	359.73	384.13	334.42	0.014	0.007	0.004	0.002
10	110.7	5.95	273.62	292.18	254.37	0.011	0.005	0.003	0.001

* http://physics.nist.gov/PhysRefData/XrayMassCoef/tab3.html

** Titania densities used: anatase (an) 3.98 $g.cm^2$; rutile (ru) 4.25 $g.cm^2$; amorphous (am) 3.70 $g.cm^2$

TABLE S2: Quantitative phase analysis, inclusive of the non-diffracting component that was derived from the refined weight percent of a standard alumina spike (20 wt%).

Calcination (˚C)	λ (Å)	Non-diffracting (wt%)	Anatase (wt%)	Rutile (wt%)
300	neutro	10.0_6	89.9_4	0
	1.436	7.2_1	92.7_9	0
	1.541	6.8_0	93.2_0	0
	1.659	11.0_5	88.9_5	0
	1.789	12.3_4	87.6_6	0
	1.948	13.8_7	86.1_3	0
400	neutro	7.7_3	92.2_7	0
	1.436	8.3_1	91.6_9	0
	1.542	5.7_9	94.2_1	0
	1.659	12.5_0	87.5_0	0
	1.789	14.0_7	85.9_3	0
	1.938	19.1_5	80.8_5	0
	2.102	21.0_4	78.9_6	0
	2.290	22.3_8	77.6_2	0
500	1.436	15.0_5	84.9_5	0
	1.542	18.1_0	81.9_0	0
	1.659	22.7_7	77.2_3	0
	1.790	23.0_4	76.9_6	0
	1.938	24.1_1	75.8_9	0
	2.102	24.4_9	75.5_1	0
	2.291	33.7_6	66.2_4	0
600	neutro	8.8_2	72.5_4	18.6_4
	1.435	30.6_7	55.7_5	13.5_8
	1.540	32.2_8	54.9_0	12.8_2
	1.658	35.2_9	52.4_5	12.2_6
	1.790	41.5_1	46.9_4	11.5_5
	1.936	45.9_1	43.6_0	10.4_8
	2.102	47.1_6	42.0_3	10.8_1
	2.291	51.4_6	40.2_9	8.2_5
800	1.436	44.1_4	0	55.8_6
	1.241	47.1_1	0	52.8_9
	1.659	52.1_9	0	47.8_1
	1.790	56.0_4	0	43.9_6
	1.938	59.1_0	0	40.9_0
1000	neutro	10.2_8	0	89.7_2
	1.435	49.1_1	0	50.8_9
	1.541	53.9_1	0	46.0_9
	1.658	57.7_2	0	42.2_8
	1.789	61.5_7	0	38.4_3
	1.937	64.3_3	0	35.6_7
	2.101	68.3_1	0	31.6_9
	2.290	71.4_5	0	28.5_5

TABLE S3: Attenuation of anatase and rutile wt% derived from the Rietveld scale factors as function of X-ray energy. For each temperature, the absolution attenuation was estimated from the $I/I_o = e^{-\mu t}$ for crystals fixed to the Rietveld refined size determined at E = 8.64 keV, and this correction applied for all energies.

5

Calcination (°C)	Rietveld Crystal Size (nm)	E (keV)	λ (Å)	Anatase			Rutile		
				wt%	Rel. Atten.	Abs. Atten.	wt%	Rel. Atten.	Abs. Atten.
300	**7**	6.40	1.936	78.46	0.996	0.996			
		6.93	1.790	78.70	0.999	0.999			
		7.48	1.658	78.15	0.992	0.992			
		8.05	1.540	79.22	1.005	1.005			
		8.64	1.453	78.81	1.000	1.000			
400	**10**	6.40	1.936	76.23	0.968	0.967			
		6.93	1.790	78.55	0.997	0.996			
		7.48	1.658	78.53	0.997	0.996			
		8.05	1.540	79.38	1.007	1.006			
		8.64	1.453	78.79	1.000	0.999			
500	**19**	6.40	1.936	75.85	0.974	0.964			
		6.93	1.790	76.09	0.977	0.967			
		7.48	1.658	76.33	0.980	0.970			
		8.05	1.540	77.21	0.992	0.982			
		8.64	1.453	77.85	1.000	0.990			
600	**40/122**	6.40	1.936	56.16	0.936	0.916	13.61	0.925	0.861
		6.93	1.790	57.09	0.952	0.932	14.18	0.963	0.899
		7.48	1.658	59.43	0.991	0.971	13.99	0.950	0.886
		8.05	1.540	60.18	1.003	0.983	14.14	0.961	0.897
		8.64	1.453	59.99	1.000	0.980	14.72	1.000	0.936
800	**330**	6.40	1.936				64.07	0.904	0.740
		6.93	1.790				65.72	0.927	0.763
		7.48	1.658				67.58	0.954	0.790
		8.05	1.540				69.54	0.981	0.817
		8.64	1.453				70.86	1.000	0.836
1000	**400**	6.40	1.936				60.84	0.883	0.764
		6.93	1.790				62.62	0.909	0.789
		7.48	1.658				64.87	0.942	0.822
		8.05	1.540				66.69	0.968	0.848
		8.64	1.453				68.90	1.000	0.881

TABLE S4: Linear absorption co-efficients for anatase and rutile. Mass attenuation was calculated using a fixed particle size (D) of 0.01 micron and plotted against the Rietveld phase proportion (Figure 4). Changing D altered the spread of the wt% as a function of energy, but did not change the intercept when $\exp^{(\Delta\mu)D} = 1$ and microabsorption was absent. For the core-shell 5microstructures observed $\Delta\mu$ is negative for the shielded phases (anatase and rutile) and positive for the accessible phase (primary gel or aperiodic intermediate).

300°C

Energy	μan	μam	μam - μan	D (micron)	exp(Δμ)t	wt %
6.4	961.47	893.83	-67.64	0.01	0.9993	86.13
6.92	840.75	781.6	-59.15	0.01	0.9994	87.66
7.47	622.32	578.54	-43.78	0.01	0.9996	88.95
8.04	460.38	427.99	-32.39	0.01	0.9997	93.2
8.63	396.74	368.83	-27.91	0.01	0.9997	92.79

Energy	μan	μam	μan - μam	D (micron)	exp(Δμ)t	wt %
6.4	961.47	893.83	67.64	0.01	1.0007	13.87
6.92	840.75	781.6	59.15	0.01	1.0006	12.34
7.47	622.32	578.54	43.78	0.01	1.0004	11.05
8.04	460.38	427.99	32.39	0.01	1.0003	6.8
8.63	396.74	368.83	27.91	0.01	1.0003	7.21

400°C

Energy	μan	μam	μam - μan	D (micron)	exp(Δμ)t	wt %
5.41	1449.75	1347.76	-101.99	0.01	0.9990	77.62
5.9	1139.7	1059.52	-80.18	0.01	0.9992	78.96
6.4	961.47	893.83	-67.64	0.01	0.9993	80.85
6.92	840.75	781.6	-59.15	0.01	0.9994	85.93
7.47	622.32	578.54	-43.78	0.01	0.9996	87.5
8.04	460.38	427.99	-32.39	0.01	0.9997	94.21
8.63	396.74	368.83	-27.91	0.01	0.9997	91.69

Energy	μan	μam	μan - μam	D (micron)	exp(Δμ)t	wt %
5.41	1449.75	1347.76	101.99	0.01	1.0010	22.38
5.9	1139.7	1059.52	80.18	0.01	1.0008	21.04
6.4	961.47	893.83	67.64	0.01	1.0007	19.15
6.92	840.75	781.6	59.15	0.01	1.0006	14.07
7.47	622.32	578.54	43.78	0.01	1.0004	12.5
8.04	460.38	427.99	32.39	0.01	1.0003	5.79
8.63	396.74	368.83	27.91	0.01	1.0003	8.31

500°C

Energy	μan	μam	μam - μan	D (micron)	exp(Δμ)t	wt %
5.41	1449.75	1347.76	-101.99	0.01	0.9990	66.24
5.9	1139.7	1059.52	-80.18	0.01	0.9992	75.51
6.4	961.47	893.83	-67.64	0.01	0.9993	75.89
6.92	840.75	781.6	-59.15	0.01	0.9994	76.96
7.47	622.32	578.54	-43.78	0.01	0.9996	77.23
8.04	460.38	427.99	-32.39	0.01	0.9997	81.9
8.63	396.74	368.83	-27.91	0.01	0.9997	84.95

Energy	μan	μam	μan - μam	D (micron)	exp(Δμ)t	wt %
5.41	1449.75	1347.76	101.99	0.01	1.0010	33.76
5.9	1139.7	1059.52	80.18	0.01	1.0008	24.49
6.4	961.47	893.83	67.64	0.01	1.0007	24.11
6.92	840.75	781.6	59.15	0.01	1.0006	23.04
7.47	622.32	578.54	43.78	0.01	1.0004	22.77
8.04	460.38	427.99	32.39	0.01	1.0003	18.1
8.63	396.74	368.83	27.91	0.01	1.0003	15.05

600°C

Energy	μan	μam	μam - μan	D (micron)	exp(Δμ)t	wt %
5.41	1449.75	1347.76	-101.99	0.01	0.9990	40.29
5.9	1139.7	1059.52	-80.18	0.01	0.9992	42.03
6.4	961.47	893.83	-67.64	0.01	0.9993	43.6
6.92	840.75	781.6	-59.15	0.01	0.9994	46.94
7.47	622.32	578.54	-43.78	0.01	0.9996	52.45
8.04	460.38	427.99	-32.39	0.01	0.9997	54.9
8.63	396.74	368.83	-27.91	0.01	0.9997	55.75

Energy	μru	μam	μan - μru	D (micron)	exp(Δμ)t	wt %
5.41	1548.1	1347.76	-200.34	0.01	0.9980	8.25
5.9	1217.02	1059.52	-157.5	0.01	0.9984	10.81
6.4	1026.69	893.83	-132.86	0.01	0.9987	10.48
6.92	897.79	781.6	-116.19	0.01	0.9988	11.55
7.47	664.54	578.54	-86	0.01	0.9991	12.26
8.04	491.62	427.99	-63.63	0.01	0.9994	12.82
8.63	423.66	368.83	-54.83	0.01	0.9995	13.58

Energy	μan	μam	μan - μam	D (micron)	exp(Δμ)t	wt %
5.41	1449.75	1347.76	101.99	0.01	1.0010	51.46
5.9	1139.7	1059.52	80.18	0.01	1.0008	47.16
6.4	961.47	893.83	67.64	0.01	1.0007	45.91
6.92	840.75	781.6	59.15	0.01	1.0006	41.51
7.47	622.32	578.54	43.78	0.01	1.0004	35.29
8.04	460.38	427.99	32.39	0.01	1.0003	32.28
8.63	396.74	368.83	27.91	0.01	1.0003	30.67

Energy	μru	μam	μan - μru	D (micron)	exp(Δμ)t	wt %
5.41	1548.1	1347.76	200.34	0.01	1.0020	51.46
5.9	1217.02	1059.52	157.5	0.01	1.0016	47.16
6.4	1026.69	893.83	132.86	0.01	1.0013	45.91
6.92	897.79	781.6	116.19	0.01	1.0012	41.51
7.47	664.54	578.54	86	0.01	1.0009	35.29
8.04	491.62	427.99	63.63	0.01	1.0006	32.28
8.63	423.66	368.83	54.83	0.01	1.0005	30.67

800°C

Energy	μru	μam	μam - μru	D (micron)	exp(Δμ)t	wt %
6.4	1026.69	893.83	-132.86	0.01	0.9987	40.9
6.92	897.79	781.6	-116.19	0.01	0.9988	43.96
7.47	664.54	578.54	-86	0.01	0.9991	47.81
8.04	491.62	427.99	-63.63	0.01	0.9994	52.89
8.63	423.66	368.83	-54.83	0.01	0.9995	55.86

Energy	μru	μam	μan - μru	D (micron)	exp(Δμ)t	wt %
6.4	1026.69	893.83	132.86	0.01	1.0013	59.1
6.92	897.79	781.6	116.19	0.01	1.0012	56.04
7.47	664.54	578.54	86	0.01	1.0009	52.19
8.04	491.62	427.99	63.63	0.01	1.0006	47.11
8.63	423.66	368.83	54.83	0.01	1.0005	44.14

1000°C

Energy	μru	μam	μam - μru	D (micron)	exp(Δμ)t	wt %
5.41	1548.1	1347.76	-200.34	0.01	0.9980	28.55
5.9	1217.02	1059.52	-157.5	0.01	0.9984	31.69
6.4	1026.69	893.83	-132.86	0.01	0.9987	35.67
6.92	897.79	781.6	-116.19	0.01	0.9988	38.43
7.47	664.54	578.54	-86	0.01	0.9991	42.28
8.04	491.62	427.99	-63.63	0.01	0.9994	46.09
8.63	423.66	368.83	-54.83	0.01	0.9995	50.89

Energy	μru	μam	μan - μru	D (micron)	exp(Δμ)t	wt %
5.41	1548.1	1347.76	200.34	0.01	1.0020	71.45
5.9	1217.02	1059.52	157.5	0.01	1.0016	68.31
6.4	1026.69	893.83	132.86	0.01	1.0013	64.33
6.92	897.79	781.6	116.19	0.01	1.0012	61.57
7.47	664.54	578.54	86	0.01	1.0009	57.72
8.04	491.62	427.99	63.63	0.01	1.0006	53.91
8.63	423.66	368.83	54.83	0.01	1.0005	49.11

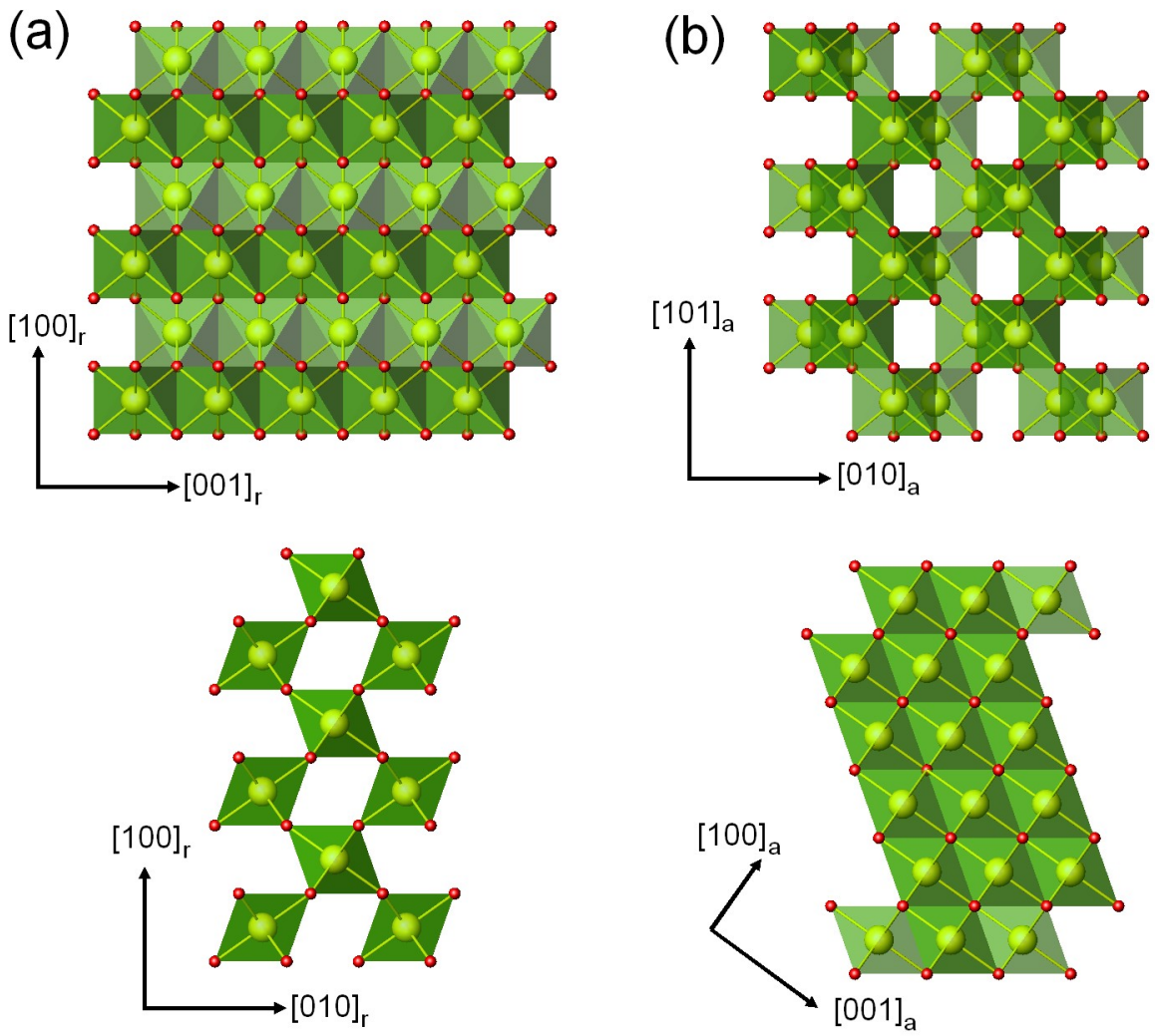

FIGURE S1. (a) Rutile and (b) anatase represented as ideal TiO_6 octahedra and emphasizing the 5relationship between the close-packed planes that allow topotaxial interfaces, but which play an indirect role during phase interconversion as the transformation is mediated by an aperiodic intermediate compound.

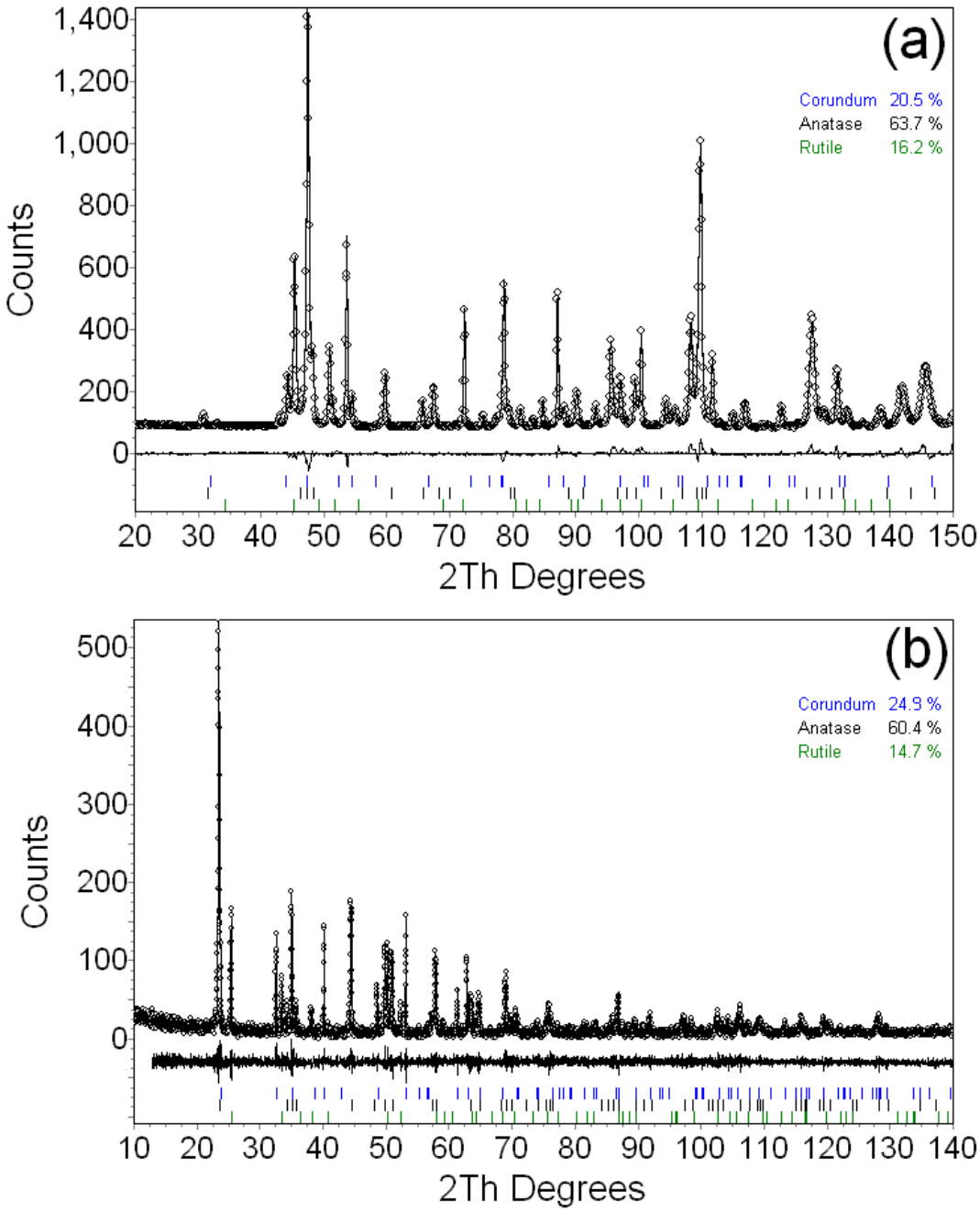

FIGURE S2. Rietveld plots for sol gel derived titania fired at 600°C for 2 hours and spiked with 20 wt% alumina as an internal standard. (a) Neutron data collected at λ = 1.911 Å (with a value of goodness of fit, GOF = 0.48). (b) Synchrotron X-ray data collected at λ = 1.435 Å (with a 5GOF value of 1.04).